Thin films for CIS solar cells

M. Abd-Lefdil, C. Messaoudi, H. Bihri, S. Abd-Lefdil and D. Sayah
Laboratory of materials physics, physics department, faculty of sciences
P.B. 1014, Rabat-Morocco

In this paper, we present our Studies on three materials $CuInS_2$, ZnO and CdS which can be used to elaborate CIS solar cells. For instance, we have used spray pyrolysis and chemical bath deposition to prepare these compounds. Sprayed $CuInS_2$ thin films have exhibited a preferential(112) orientation with chalcopyrite structure and p type conductivity. Their energy gap value was around 1.45 eV, which perfectly matches the solar spectrum. We also studied the Cu:In :S ratio effect on its properties.
Sprayed Undoped and indium-doped ZnO films were highly transparent since their energy gap value was 3.2 eV. The films were polycrystalline and exhibited an hexagonal wurtzite-type structure. Their orientation was modified by an adequate indium doping which leads to a resistivity value of about 10^{-3} Ωcm.
Homogeneous and strongly adherent CdS very thin layers of about 70 nm were prepared by CBD Process. The obtained films have showed preferential orientation which changes from (002) to (101) with growth temperature and annealing treatment. CdS was very resistive with an energy gap around 2.37 eV.

PACS numbers : 68.55.a

I. INTRODUCTION

Three semiconductors materials are the main candidates for thin film solar cells : amorphous silicon a-Si, cadmium telluride CdTe and $Cu(In,Ga)(S,Se)_2$ abbreviated CIS. Each of these materials has its own advantages and disadvantages as it has been reported in details by Schock [1].

Our attention was focused on CIS materials and especially on $CuInS_2$ ternary compound. $CuInS_2$ is one of a promising interest for photovoltaic applications due to its band gap of 1.53 eV [2] which perfectly matches the solar spectrum. Furthermore, solar conversion efficiency of 10.8 % [3] was obtained by associating $CuInS_2$ to CdS/ZnO bilayer.

In this paper, we report our studies on $CuInS_2$ and ZnO films prepared by spray pyrolysis. We also present our results on CdS prepared by chemical bath deposition process. These compounds will be used later on solar cells fabrication.

As all of I-III-IV_2 ternary compounds, a number of potential defects are considered (points defects, crystal defects, grains boundaries..) [4]. Intrinsic defects resulting from non stoichiometry films such as cation vacancies and anti-site defects play an important role on $CuInS_2$ conductivity type (n or p) and its physical properties [5]. Furthermore, many secondary phases appear in the deposited layers such as Cu_2S and In_2S_3. This apparition depends on the used technique [6].

Several techniques including chemical vapour transport [6], three sources molecular beam epitaxy [7], sulfurisation [8], electrodeposition [9], r.f. sputtering [10] and spray pyrolysis [11,12] have been used to prepare $CuInS_2$ layers.

Zinc oxide ZnO is one of binary transparent semiconductors, which has attracted great interest due to its potential performance in optoelectronic and photovoltaic applications. A wide variety of preparation techniques, using different source, has been used to prepare ZnO films such as reactive evaporation [13], spray pyrolysis [14], metal organic chemical vapour deposition [15], r.f sputtering [16] and chemical vapour deposition [17] . .

Cadmium sulfide CdS was prepared in the past years by many techniques such as for ZnO. But since few years, chemical bath deposition (CBD) [18,21] was used for preparing very thin films of CdS for avoiding chemistry interfacial problem in CdS (n)-Absorber (p) heterojunctions. Furthermore, Britt et al [20] have obtained recently 15.8 % solar conversion efficiency in CdS(CBD)-CdTe photovoltaic cells while Braunger et al [3] have obtained 10.8 % in ZnO/CdS(CBD)/$CuInS_2$ devices.

II. EXPERIMENTAL PROCEDURE

By using various copper sources such as CuCl, $Cu(CH_3COO)_2$-H_2O or $CuCl_2$-$2H_2O$ in the starting spray solution, we have showed that hydrated cupric chloride gave the best results [22].

Aqueous solutions of hydrated cupric chloride $CuCl_2$-$2H_2O$, indium chloride $InCl_3$ and thiourea $CS(NH_2)_2$ were prepared by dissolving appropriate amounts in deionised water and sprayed onto heated glass substrates using air as carrier gas. The spray solution was prepared for different Cu:In ratios and with sulphur excess of stoichiometry since S is very volatile. Details of experiments are reported elsewhere [23][24].

For ZnO layers, the spraying solution consists of 0.05 M of zinc chloride $ZnCl_2$ dissolved in deionized water. For indium doping, $InCl_3$ was added to the starting solution. A few drops of acetic acid were systematically added to increase the clarity of the starting solution by dissolving precipitates. The optimum spraying conditions are reported in previous papers [25] [26].

Preparation of CdS by CBD process is based on the decomposition of thiourea in ammonia solution containing dissolved cadmium ions. Our details of experiments have been recently published [27].

The crystalline properties and surface morphology were respectively examined by X-Ray Diffraction (XRD) analysis and Scanning Electron Microscopy (SEM). Electron Probe MicroAnalysis (EPMA) was used to determine the film composition. Electrical properties were determined from thermoelectric, Hall effect and Van Der

 © 1998 The Morrocan Statistical Physical Society

Paw techniques while optical measurements were taken at 300 K in visible and near infrared wavelength range.

III. RESULTS AND DISCUSSION

A-$CuInS_2$ films

EPMA analysis showed that the film composition did not agree with the mixture composition of the spray solution as it is reported in the table below.

Initial ratio Cu:In:S	Cu (at %) in the film	In (at %) in the film	S (at %) in the film
0.8:1:3	26.1	27.1	46.8
0.9:1:3	28.2	25.6	46.2
1.0:1:3	29.6	24.4	46.0
1.1:1:3	31.5	21.4	47.1
1.2:1:3	36.7	19.6	43.7
1.3:1:3	39.7	18.7	41.6
1.0:1:3	29.6	24.4	46.0
1.0:1:4	28.8	25.0	46.2
1.0:1:5	28.5	25.2	46.3
1.0:1:6	25.9	24.8	49.3

We also note that Cu:In ratio is higher than the ratio in the solution and the stoichiometry is improved when the S content is increased. We also note that S:Cu ratio increases less rapidly that S:In when S content increases in the initial solution [24]. This result can be interpreted as sulphur scavenging of both Cu and In atoms in $CuInS_2$ matrix, which is more important for Cu atoms. This behaviour has also been observed for $CuInS_2$ after annealing under H_2S atmosphere [28] while Watanabe et al [29] have reported that precursors containing enough S atoms suppress the aggregation of In atoms on the film surface.

XRD patterns of films sprayed at different Cu:In:S ratios in the initial solution and deposited on glass substrate are presented in figure 1. They indicate the formation of polycrystalline $CuInS_2$ films with a preferred (112) orientation. The existence of the (103) line indicates the chalcopyrite structure of the film. The crystallographic parameters computed from XRD patterns were $a \approx 0.552$ nm and $c \approx 1.122$ nm. However, it appears that increasing the Cu:In ratio up to 1.2 favours the formation of Cu_2S secondary phase while sulphur-rich initial solution leads to an additional peak attributed to In_2S_3 secondary phase.

All of the obtained films were p type semiconductors. Thus making them suitable for heterojunctions solar cells with n type semiconductors. Resistivity, carrier density N_A and hole mobility μ_p at room temperature in the dark are presented in the next table.

Initial ratio Cu:In:S	ρ (Ωcm)	N_A cm^{-3}	$\mu_p cm^2V^{-1}s^{-1}$
0.9:1:3	63	$3.8\ 10^{16}$	2.6
1.0:1:3	2.0	$2.7\ 10^{17}$	11.6
1.1:1:3	$6.0\ 10^{-2}$	$1.8\ 10^{19}$	5.8
1.2:1:3	$2.8\ 10^{-2}$	$9.0\ 10^{19}$	2.5
1.0:1:4	10	-	-
1.0:1:5	10^2	-	-
1.0:1:6	10^3	-	-

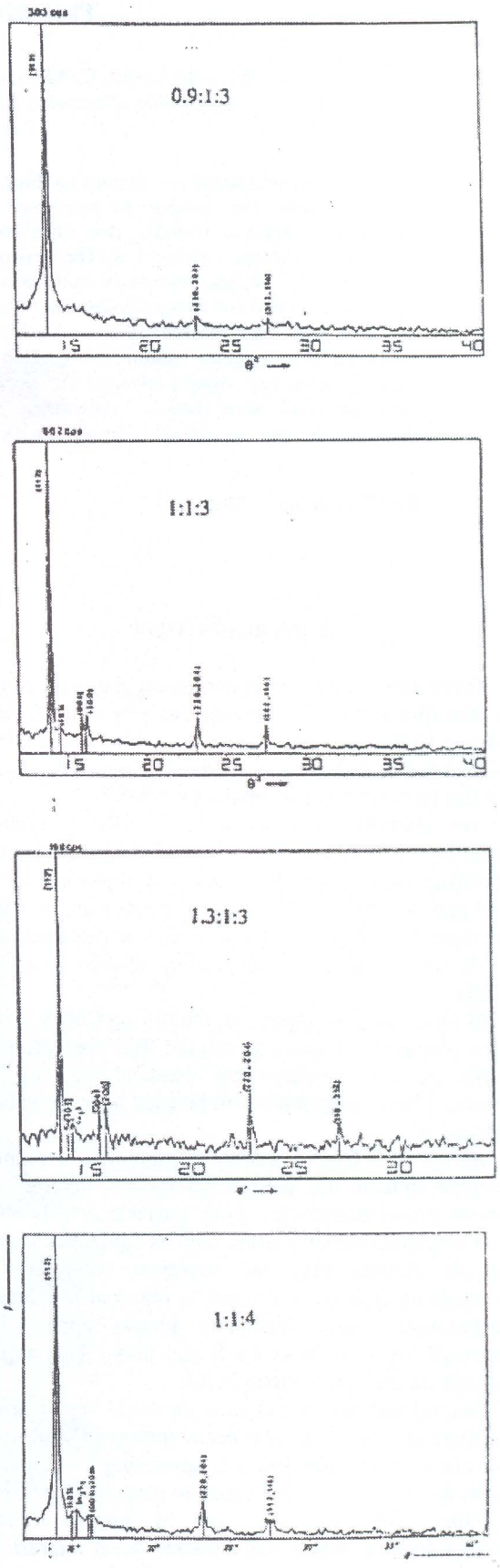

FIG.1: X-ray diffraction patterns of $CuInS_2$ thin films deposited at different ionic Cu:In:S ratios in the initial spray solution.

One can note that the resistivity value depends on the initial Cu:In:S ratio. High Cu:In ratio leads to a low resistivity and a mobility value comparable to p type $CuInS_2$ single crystal [33]. This lowest mobility observed for films deposited with copper in excess would be expected to yield a higher carrier concentration. The above signalled scavenger of Cu atoms by the sulphur reduces the carriers density and leads to an increase in resistivity. However, it was difficult to determine μ_p and N_A for resistive films since the hall voltage was very small.

From our SEM micrographs [23][30], the average grain size was around 50 nm and numerous particles of a diameter in the range 100 to 500 nm were present in the film surfaces. Their density depends on the initial Cu:In:S ratios. These results are in a good agreement with literature [31][32].

Figures 2 and 3 show the transmission T spectra as a function of wavelength for $CuInS_2$ thin films sprayed at different Cu:In:S ratios in the initial solution. The absorption coefficient α is calculated from these curves using Wemple and Seman method [34]. Extrapolation of $(\alpha h\upsilon)^2$ against the photon energy $h\upsilon$ curves lead to the band gap energy.

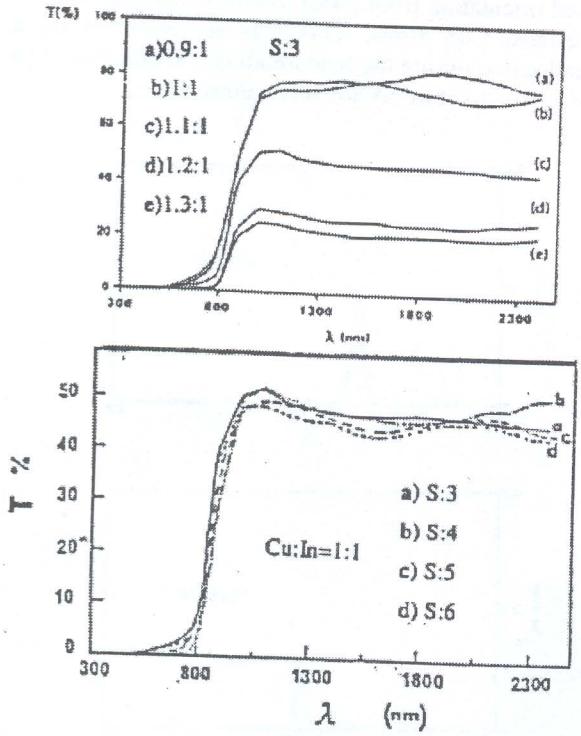

FIG.2,3: Transmission spectra of $CuInS_2$ thin films deposited at different Cu:In ratios and different s contents.

T spectra for films deposited with various amounts of excess copper in the spray solution (fig.2) show that transmission decreases from 80 % to 20 % when Cu:In ratio increases from 0.8 to 1.3. One can note the absence of interference fringes which is in agreement with the surface topography.

For films prepared with an excess of sulphur (fig.3), the transmission is around 50 % in 2300-1000 nm wavelength range which is explained by the importance of the reflection due to the surface aspect. We also observe that interference fringes appear and become more contrasted when S content increases. This result is in agreement with the evolution of the morphology since the grain size increases. These spectra display a single slope in the absorption edge region of 800-1000 nm. α was around 10^4 cm^{-1} near the band edge due to an allowed direct transition.

The obtained gap values were around 1.45 eV. So, it lies in the optimum range for solar conversion and leads $CuInS_2$ to act as an absorber material in solar cells devices. Moreover, this gap value is less than 1.53 eV reported elsewhere [2].

B- ZnO films

XRD spectra of undoped and 2 at % indium doped ZnO films by using zinc chloride are shown in figure 4.

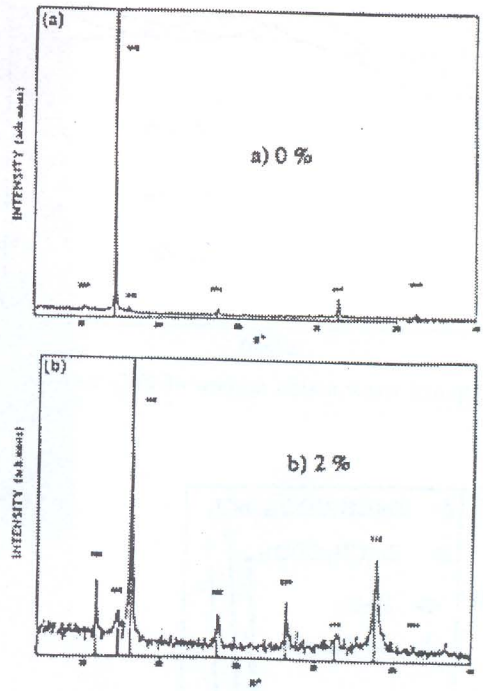

FIG.4: X-ray spectra of ZnO films with different In:Zn ratios.

All the as-deposited films were polycrystalline and exhibited hexagonal wurtzite structure. According to these diffractograms, the c-axis orientation of the film structure was significantly modified by the indium doping. Therefore, no additional peak (other than expected for ZnO) was observed . For undoped ZnO, a preferred orientation of the c-axis (002) perpendicular to the substrate was observed as shown in figure ?.For indium-doped ZnO, the (101) peak had the maximum intensity, which leads to to another preferred orientation of crystallites. A similar effect was observed with the znO layers obtained by using zinc acetate as source compound. These results are in good agreement with literature [35].

SEM micrographs of the surface morphology of the undoped and doped ZnO films [25,26] show that the obtained films display two uniform and distinct

Morphologies. For the films obtained by using zinc chloride, the surface shows a tetrahedral morphology with typical grain size of about 10^3 nm. With indium doping, the tetrahedral morphology becomes more dense and the grain size decreases. A similar surface aspect has been observed on ZnO films prepared by MOCVD [36]. On the other hand, for films obtained by using acetate, the surface aspect was remarkably less pronounced with very grain size , which decreases after an indium doping.

The optical transmission curves of the undoped and indium-doped ZnO are shown in figure 5. All the films were found to be highly transparent (80 to 90 %) in the visible range with a sharp absorption edge at about 380 nm the light diffusion, which we related to the surface aspect and the small crystallite size. In order to study the source compound and the indium doping effect on the band gap energy E_g, the squared absorption coefficient versus photon energy was represented in figure 6. One can note that no significant effect on E_g occurs since it lies in 3.17-3.27 eV range.

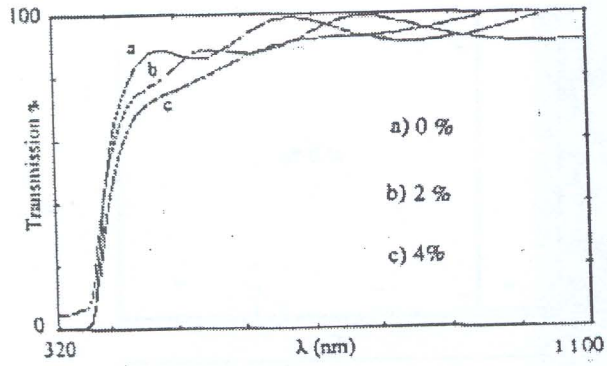

FIG. 5: Optical transmission spectra of ZnO with different In:Zn ratios.

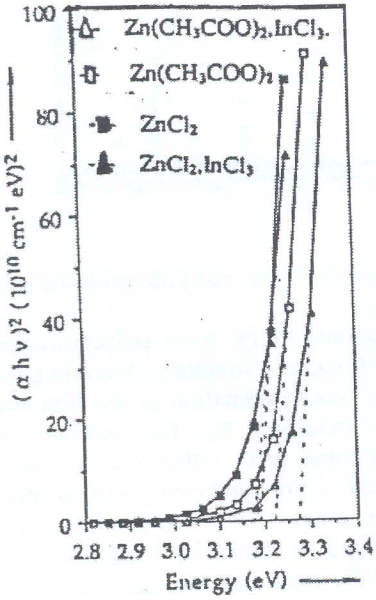

FIG.6: (αhυ) vs hυ plots for undoped and doped ZnO films.

In a table below, we compare our results on resistivity measurements obtained to literature.

Synthesis technique	ρ Ωcm	reference
spray (In)	10^{-3}	14
spray (Al)	$2\ 10^{-3}$	37
spray	$2\ 10^{-4}$	38
sputtering	10^{-2} to 10^{-4}	39
spray	10 to 10^{-1}	this work
spray (In)	10^{-3}	this work

One can note that after indium doping with a concentration of 2 at %, the conductivity increases approximately by two orders of magnitude.

C- CdS films

Homogeneous and strongly adherent CdS very thin films of about 70 nm were found to be polycrystalline with an hexagonal structure. However, the samples grown at 70 °C exhibit a dominant (002) preferred orientation, which changes when the growth temperature increases to 80 and 90 °C, where (101) is the preferred orientation (fig.7). (101) peak intensity increases with the growth temperature in agreement with Borges et al results [19].

After an annealing treatment in air for one hour at 350 °C, the same phenomenon about the change in the preferred orientation from (002) to (101) was observed for the annealed CdS films. This can be explained by a recrystallisation during the heat treatment, which leads to a change in the structure parameters values.

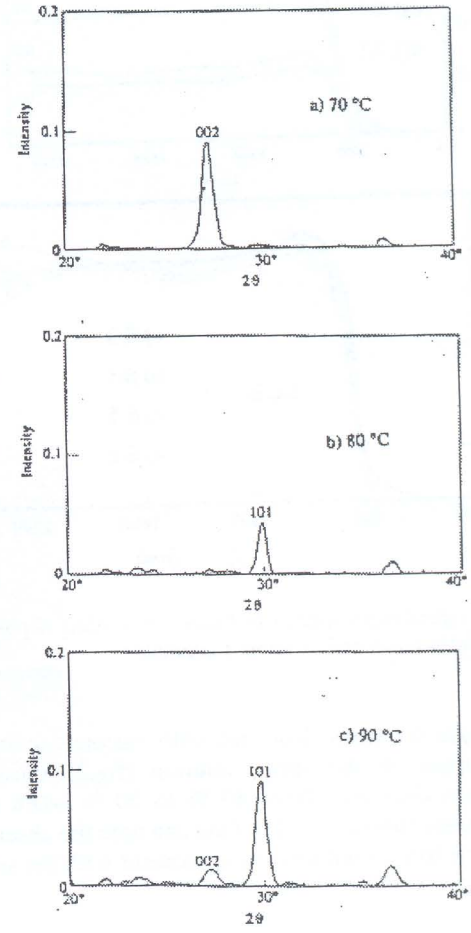

FIG. 7: X ray diffraction patterns for CdS prepared by CBD process at different growth temperatures.

Spherical features were observed in CdS (CBD) surface by SEM for lower temperature (70 °C.Up to this temperature (at 90 °C), the spherical features becomeless numerous and microcrystallites occur [27].

Transmission measurements (fig.8) have showed the absence of interference fringes due to the diffuse light scattering in agreement with the surface topography and the crystallite size. from $(\alpha h\upsilon)^2$ versus $h\upsilon$, the gap energy was around 2.37 eV, less lower than the usual accepted value 2.42 eV.

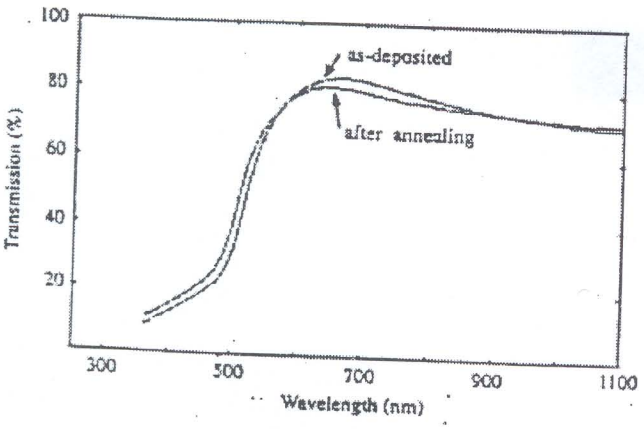

FIG.8:Transmission spectra for CdS (CBD) as deposited and after an annealing treatment.

All of the obtained CdS films were n type conductivity and highly resistive with room temperature resistivity of about 10^7 Ωcm, in the range of values reported in the literature [21][40]. This is due to the very low crystallite sizes which lead to very high density of grains boundaries. These defects are the privileged sites for oxygen adsorption and form an energy barrier for the carriers motion.

IV. CONCLUSION

The spray pyrolysis was shown to be a simple method for producing single phase $CuInS_2$ thin films with chalcopyrite structure. The sprayed films with excess sulphur were nearly stoichiometric and have p type conductivity and a direct band gap of about 1.45 eV. So, it can be used as an absorber material in photovoltaic devices.

Transparent conducting and uniform sprayed undoped and induim-doped ZnO layers were prepared. Their energy gap value was around 3.2 eV and the resistivity lied between 10^{-2} and 10^{-3} Ωcm after 2 at % indium doping. So, ZnO can act as a conducting transparent electrode instead of the usual ITO layers.

CdS very thin films prepared by CBD process were homogeneous and strongly adherent. They were n type semiconductors, very resistive and presented high optical transmission with an energy gap value of about 2.37 eV, which leads this semiconductor to act as an optical window in photovoltaic cells.

These three compounds are very adapted to elaborate $CuInS_2$/ZnO/CdS CIS solar cells.

[1] H.W. Schock, Appl. Surface Science 92, 606 (1996).
[2] J.L. Shay and J.H. Wernick, Ternary Chalcopyrite Semiconductors: Growth, Electronic Properties and Applications, Pergamon Press, New York, 1976.
[3] D. Braunger, D. Hariskos, T. Walter and H.W. Schock, Solar Energy Mater. Solar Cells 40, 97 (1996).
[4] A. Rockett et al, Thin solid films 237, 1 (1994)
[5] T. Yamamoto and H. Katagama-Yoshida, Jpn. J. Apll. Phys. 34, L 1584 (1995).
[6] M.J. Tafreski, K. Balakrishnan and R. Dhanasekaran, Nuovo cimento della societa Italiana di fisica, 18-4, 471 (1996).
[7] S. Niki, P.J. Fons, A. Yamada, T. Kurafuji, S. Chichiba, W.G. Bi and C.W. Tu, Appl. Phys. Lett. 69, 647 (1996).
[8] Y. Ogawa, A. Jagerwaldan, T.H. Hua, Y. Hashimoto and K. Ito, Appl. Surf. Sci. 92, 232 (1996).
[9] T. Yukawa, K. Kuwabara and K. Koumoto, Thin Solid Films 280, 160 (1996).
[10] Y. Yamamoto, T. Yamaguchi, Y. Denizu, T. Tanaka and A. Yoshida, Thin Solid Films 281-282, 372 (1996).
[11] A.N. Tiwari, D.K. Pandya and K.L. Chopra, Solar Energy Mater. Solar Cells 40, 97 (1996).
[12] B. Pamplin and R.S. Fiegelson, Thin Solid Films 60, 141 (1979).
[13] D.E. Brodie, R. Singh, J.H.Morgans, J.D. Leslie, L.J. Moore and A.E. Diwon, Proc. 14th IEEE Photovoltaic Specialists Conf., San Diego (CA) P.468 (1980).
[14] S. Major, A. Banerjee and K.L. Chopra, Thin Solid Films 108, 333 (1983).
[15] W.W. Wenas, A. Yamada, M. Konagai and K. Takahashi, Jap.J.Appl.Phys. 30, 441 (1991).
[16] L. Vasanelli, A. Valentini and A. Lasacco, Solar energy Mater. 16, 91 (1987).
[17] A.P. Roth and D.F. Williams, J.Appl.Phys.52, 6685 (1981).
[18] W.J. Danaher, L.E. Lyons and G.C. .Morris, Solar Energy Mater. 12, 137 (1985).
[19] R.O. Borges and D. Lincot, J. Electrochem. Soc. 140, 3464 (1993).
[20] J. Britt and C. Ferekides, Appl.Phys.Letters 62, 2851 (1993).
[21] O .de Melo, L. Hernandez, O. Zelaya-Angel, R. Lozada-Morales, M. Becerril and E. Vasco, Appl.Phys.Letters 65, 1278 (1994).
[22] C. Messaoudi, H. Bihri D. Sayah, M. Cadene and M. Abd-Lefdil, J.Mater. Sci. Letters 11, 1234 (1992).
[23] H. Bihri, C. Messaoudi, D. Sayah, A. Boyer, A. Mzerd and M. Abd-Lefdil, Phys. Status Solidi (a) 129, 193 (1992).
[24] H. Bihri and M. Abd-Lefdil, Thin Solid Films (Submitted June 1998).
[25] C. Messaoudi, D. Sayah, and M. Abd-Lefdil, Phys. Status solidi (a) 151, 93 (1995).
[26] C. Messaoudi, S. Abd-Lefdil, D. Sayah and M. Cadene, Eur.Phys.J.AP 1, 181 (1998).
[27] S. Abd-Lefdil, C. Messaoudi, M. Abd-Lefdil and D. Sayah, Phys. Status solidi (a) 168, 417 (1998).
[28] R. Scheer,I. Luck, H. Sehnert and H.G. lewerenz, Solar Energy Mater. Solar Cells 41-42, 261 (1996).
[29] T. Watanabe and M. Matsui,Jap.J.Appl.Phys. 35, L681 (1996).
[30] H.Bihri, C. Messaoudi, D. Sayah, and M. Abd-Lefdil, Mater. Chemistry and Physics 34, 24 (1993).

[31]G.D.Padam and S.U. Rao, Solar Energy Mater. 13, 297 (1986).

[32]P.Rajaram, R.Thangarai, A.K.Sharma, A.Raza and O.P. Agnihotri, Thin Solid Films 100, 111 (1983).

[33]B. Tell, J.L. Shay and H.M. Kasper, J.Appl.Phys. 43, 2469 (1972).

[34]S.H. Wemple and J.A. Seman, Appl.Optics 12, 2947 (1973).

[35]S.Major, A. Baerjee and K.L. Chopra, Thin Solid Films 143, 19 (1986).

[36]H.Takato, M. Yamanaka, Y. Hayashi, R. Shimokawa, I. Hide, S.Gohda, F. Nagamine and T. Suboi, Jap.J.Appl.Phys. 31, 1665 (1992).

[37]A.F. Aktauruzzaman, G.L. Sharma and L.K. Malhotra, Thin Solid Films 198, 67 (1991).

[38]L.Bahadur, M. hamdani, J.F. Koening and P.Chartier, Solar Energy Mater. 14, 107 (1986).

[39]T.Minami, H. Nauto, S. Shooji and S. Takata, Thin Solid Films 111, 167 (1984).

[40] H.N. Cui and S.Q.Xi, thin Solid Films 228, 325 (1996)